ELSEVIER

Atmospheric Research 67–68 (2003) 117–133

ATMOSPHERIC RESEARCH

www.elsevier.com/locate/atmos

Proximity sounding analysis for derechos and supercells: an assessment of similarities and differences

Charles A. Doswell III[a,*], Jeffry S. Evans[b]

[a] *Cooperative Institute for Mesoscale Meteorological Studies, University of Oklahoma, 100 E. Boyd, Room 1110, Norman, OK 73019, USA*

[b] *NOAA/Storm Prediction Center, Norman, OK, USA*

Accepted 28 March 2003

Abstract

Proximity soundings (within 2 h and 167 km) of derechos (long-lived, widespread damaging convective windstorms) and supercells have been obtained. More than 65 derechos, accompanied by 115 proximity soundings, are identified during the years 1983 to 1993. The derechos have been divided into categories according to the synoptic situation: strong forcing (SF), weak forcing (WF), and "hybrid" cases (which are neither weakly nor strongly forced). Nearly 100 supercell proximity soundings have been found for the period 1998 to 2001, subdivided into nontornadic and tornadic supercells; tornadic supercells were further subdivided into those producing significant (>F1 rating) tornadoes and weak tornadoes (F0-F1 rating).

WF derecho situations typically are characterized by warm, moist soundings with large convective available potential instability (CAPE) and relatively weak vertical wind shear. SF derechos usually have stronger wind shears, and cooler and less moist soundings with lower CAPE than the weakly forced cases. Most derechos exhibit strong storm-relative inflow at low levels. In WF derechos, this is usually the result of rapid convective system movement, whereas in SF derechos, storm-relative inflow at low levels is heavily influenced by relatively strong low-level windspeeds. "Hybrid" cases collectively are similar to an average of the SF and WF cases.

Supercells occur in environments that are not all that dissimilar from those that produce SF derechos. It appears that some parameter combining instability and deep layer shear, such as the Energy–Helicity Index (EHI), can help discriminate between tornadic and nontornadic supercell

* Corresponding author.

E-mail address: cdoswell@hoth.gcn.ou.edu (C.A. Doswell).

doi:10.1016/S0169-8095(03)00047-4

situations. Soundings with significant tornadoes (F2 and greater) typically show high 0–1 km relative humidities, and strong 0–1 km shear.

Results suggest it may not be easy to forecast the mode of severe thunderstorm activity (i.e., derecho versus supercell) on any particular day, given conditions that favor severe thunderstorm activity in general. It is possible that the convective initiation mechanism is an important factor, with linear initiation favoring derechos, whereas nonlinear forcing might favor supercells. Upper-level storm-relative flow in supercells tends to be rear-to-front, whereas for derechos, storm-relative flow tends to be front-to-rear through a deep surface-based layer. However, knowing the storm-relative hodograph requires knowledge of storm motion, which can be a challenge to predict. These results generally imply that probabilistic forecasts of convective mode could be a successful strategy.

Keywords: Proximity soundings; Derechos; Supercells

1. Introduction

One of the most challenging issues confronting forecasters dealing with severe convective storms is to determine the "mode" of the anticipated convective storms. Once deep, moist convection is initiated (a challenging forecast problem in its own right), the resulting evolution can follow a wide variety of different paths: supercells, lines of convection, bow echoes, isolated muliticell storms, clusters of storms, etc. The structure and evolution of the ensuing convection is a major factor in anticipating the severe weather that might result. Supercells can produce all forms of severe weather: tornadoes, damaging winds, and large hail, whereas bow echoes are most likely to produce strong winds (although hail and tornadoes certainly can occur with bow echoes).

Recently, Evans and Doswell (2001) (hereafter referred to as ED01) presented a study of the environments of derecho-producing convective windstorms using proximity sounding analysis. An important issue in that study was the relationship between long-lasting lines of severe wind-producing storms and the low-level wind shear, since Rotunno et al. (1988) (hereafter RKW88) had hypothesized there could be a relationship useful for forecasting between low-level wind shear and the likelihood for persistent squall lines producing damaging winds. In ED01, it was shown that such storms are not limited to environments having strong low-level wind shear and large convective available potential energy (CAPE) and, therefore, whatever the merits of the RKW88 hypothesis, it apparently is not likely to be useful in forecasting long-lasting, severe wind-producing squall lines. This inconsistency between modeling studies and observed behavior was recently confirmed in a study by Gale et al. (2002).

However, in the ED01 work, there was no effort to consider the composite hodographs and thermodynamic profiles. Moreover, forecasting experience at the Storm Prediction Center (SPC) has suggested that there might be some similarities between the environments in which derechos develop and those environments giving

rise to supercells. Accordingly, there was a need to extend the study in ED01 to include an expanded treatment of the derecho data and to compare the results with a similar data set of proximity soundings for supercell storms.[1]

The data we collected are described in Section 2, and the analysis methodology is reviewed in Section 3. Results of the analysis are given in Section 4, with a discussion of the results presented in Section 5, along with a brief summary of our conclusions, including suggestions for future work.

2. Description of the data

Our data set for derechos is the same as that given in ED01, so the criteria for selecting "proximity" soundings are also the same employed in ED01: within 2 h and 167 km (100 miles) of the storm location. Unrepresentative and convectively contaminated soundings were rejected (subjectively). The derecho cases were again stratified into three categories, as in ED01: (1) weak synoptic-scale forcing (denoted as WF), (2) strong synoptic-scale forcing (denoted as SF), and (3) "hybrid" cases that did not seem to fit in either of the preceding categories.

Comparable proximity soundings for 98 discrete supercells were also collected, using the same criteria, in order to develop a comparison database. The supercells were subjectively identified using real time WSR-88D reflectivity and storm-relative velocity radar data from 1998 to 2000. A cell was determined to be a *supercell* if it maintained rotation in the 0.5° elevation scan for at least 30 min. In addition, a supercell was only included if it remained *discrete*, in order to eliminate storms embedded within extensive squall lines or derechos. All of the supercells produced one or more of the following: ≥ 2 cm (3/4 in.) diameter hail, ≥ 25 m s^{-1} (50 knot) winds, wind damage, and/or tornadoes. The supercell dataset was stratified into non-tornadic and tornadic categories. To qualify as non-tornadic, the storm must have produced severe hail and wind reports, but not a tornado report. Obviously, tornadic supercells were associated with a report of any tornado; *tornadic* supercells were again subdivided into "significant" tornadic (F2–F5 rating) and "weak" tornadic (F0–F1 rating) supercells.

Using the aforementioned criteria, 51 WF, 47 SF, and 15 Hybrid derecho proximity soundings are included in this study. In addition, 46 non-tornadic and 52 tornadic supercell proximity soundings have been used. Of the 52 tornadic supercells, 18 are associated with significant tornadoes and 34 with weak tornadoes.

Temperature and dewpoint data were collected at the surface and at 25 hPa intervals for each of the proximity soundings. In addition, the u (zonal) and v (meridional) wind components were obtained at 0.5-km intervals from the surface through 10 km AGL. The speed and direction of movement of each derecho and supercell were obtained from the radar data so that system-relative wind plots could be developed by subtracting the x

[1] An abbreviated, preliminary version of these results was presented in Evans and Doswell (2002).

and y components for each system motion from the observed wind components at each level.

3. Methodology

Several severe thunderstorm parameters were computed from each sounding, including 0–3 km AGL storm-relative helicity (SRH) as described in ED01, and the Energy–Helicity Index (EHI), which is defined as

$$\mathrm{EHI} \equiv \frac{\mathrm{CAPE} \times \mathrm{SRH}}{160{,}000},$$

where both CAPE and SRH are measured in J kg^{-1} (or, equivalently, m^2 s^{-2}), and the constant in the denominator is considered to have the same units as the numerator, so the ratio is dimensionless.[2] See Davies (1993) for a discussion of EHI.

Simple statistical analyses were performed for the various parameters and for temperature, dew point and wind component data at each level. For each of the different storm categories, skew-T, log p plots of mean temperature and dew point were constructed to estimate the degree to which the different categories had notably different thermodynamic structures. Hodograph plots were created for the means in each category and again for the 10th, 25th, 75th and 90th percentiles. For parameters based on the soundings and hodographs, box-and-whisker plots were used to illustrate the differences and similarities among the different storm categories. Although formal statistical significance testing has not yet been done, if the middle 50% of any category's distribution (i.e., between the 25th and 75th percentiles) does not overlap substantially with the middle 50% of the distribution associated with another category, then a formal test of the significance of the difference between categories is likely to reject the null hypothesis (i.e., no difference between the distributions) with a reasonably high confidence level.

4. Results

4.1. Thermodynamic profiles

A number of issues can arise constructing mean soundings; notably, there is a tendency for the detailed features in a sounding to be "smeared" such that the resulting mean sounding is smoother than the individual soundings used to derive it (see Brown, 1993). In this exploratory analysis, no attempt was made to preserve these details. Therefore, we see only the broad features within the composited soundings.

[2] EHI was introduced by J.A. Hart and W.D. Korotky in a 1991 NOAA manual for the SHARP Workstation, as referenced in ED01.

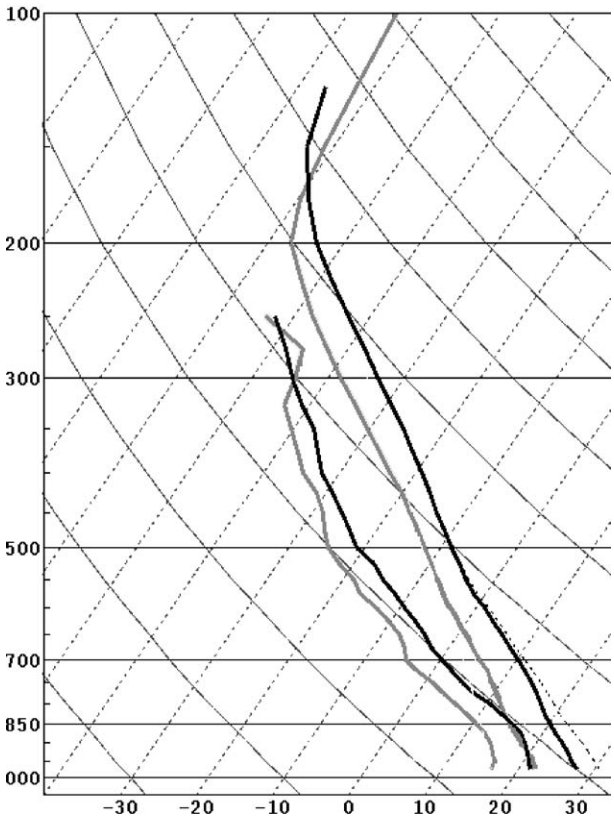

Fig. 1. Comparison skew-*T*, log *p* plots of mean temperature (right) and dewpoint (left) for WF derechos (black) and SF derechos (gray).

For the derechos, the composite sounding associated with the WF events is clearly warmer and moister than the composite for the SF events, as revealed in Fig. 1.[3] This is consistent with the findings of ED01, in which parameter studies indicated the largest buoyant instability (as measured by, CAPE) was found for WF derechos. WF events in this dataset only occurred during the warm season from May to August, whereas SF cases occurred year round and included many cool season events. Both SF and WF derecho mean soundings (Fig. 1) exhibit a dry layer and associated steep lapse rate in the mid-troposphere, which suggests the most common source region for evaporation and enhancement of the downdraft may extend from just above the boundary layer into the mid-troposphere. However, a well-mixed and dry sub-cloud layer can also support an enhanced downdraft and cold pool, with a resultant path of damaging surface winds (Corfidi, 1998).

[3] The composite sounding for the hybrid events is intermediate and, hence, is not shown.

In contrast to the derecho events, the mean soundings for tornadic versus non-tornadic supercells are very similar; there is also very little difference evident between the non-tornadic and weak tornadic events (not shown). Only the *significant* tornadic supercells exhibited clear separation from the other supercell categories (Fig. 2). The significant events have a small temperature–dew point spread from the surface through 850 hPa and somewhat reduced low-level lapse rates. When relative humidity (hereafter, RH) is examined, significant tornadic supercells occur with the highest boundary layer RH on average (Fig. 3). However, significant tornado-producing supercell cases have the greatest RH decrease between 800 and 700 hPa. In fact, the significant tornadic supercells have the lowest mean 700–500 hPa RH of the six datasets (including the derechos)! This suggests mid-level drying *alone* cannot be used to determine the potential for derechos; downdrafts might be as strong or stronger on average in significant tornadic supercells as compared to derechos, assuming evaporation is the *primary* physical process in the production of strong downdrafts (see Wakinoto, 2001). In addition, the non-tornadic supercells show the lowest mean RH through 800 hPa, followed closely by the weakly tornadic cases. This suggests boundary layer RH may be helpful in discriminating between not only tornadic and non-tornadic

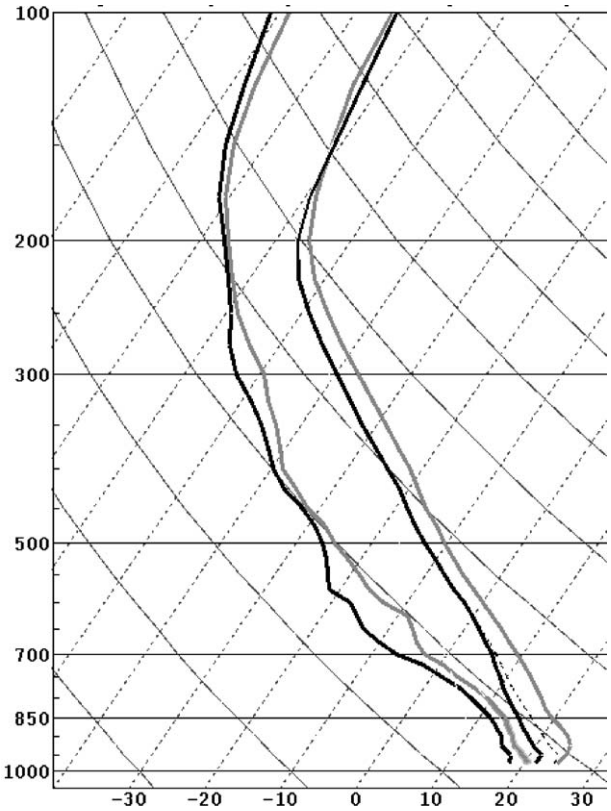

Fig. 2. As in Fig. 1, except for supercells producing significant (>F2 rating) tornadoes (black) and those producing weak (<F2 rating) tornadoes (gray).

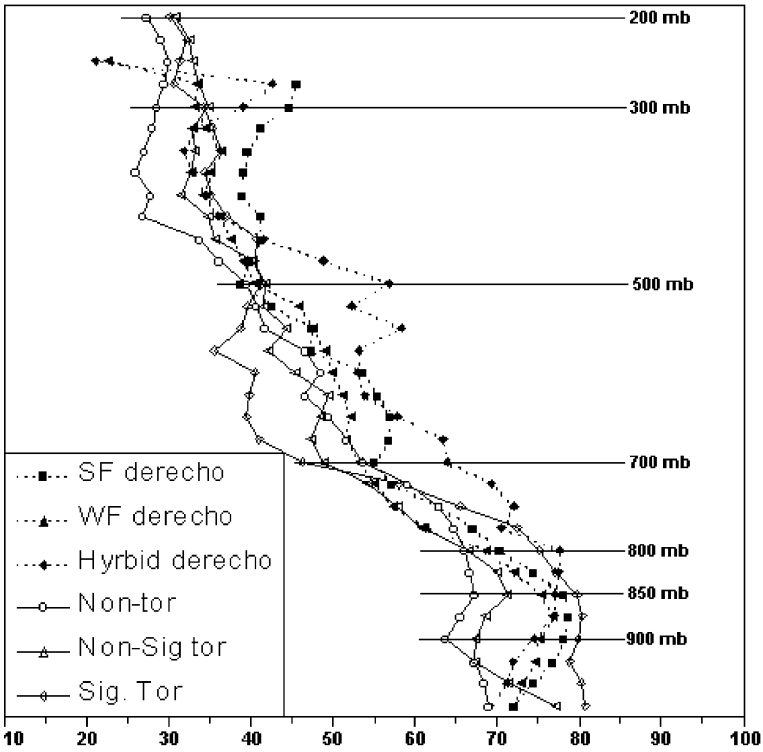

Fig. 3. Mean vertical profiles of relative humidity (percent) with pressure (hPa) for the three categories of supercells (non-tornadic, weak tornadic, and significant tornadic) and the three categories of derechos.

supercells, but also significant and weak tornadoes. Given the close association of boundary layer RH and lifting condensation level (LCL) height for surface or near-surface parcels, our findings support the belief that tornado potential and strength increase as boundary layer RH increases (i.e., LCL height decreases), as discussed in Rasmussen and Blanchard (1998), Markowski et al. (2002), and Johns et al. (2000).

Fig. 3 also shows that the low-level RH in all the derecho categories tends to *increase* with height from near the surface to about 850 hPa before decreasing above that level. One result of this characteristic is that the derecho RH profiles below 850 hPa all look more like those for significant tornado-producing supercells than like the non-tornadic or weak tornado-producing supercells. That is, derechos in our dataset tend to occur with relatively moist conditions near the surface, rather than in conditions favoring dry microbursts (Wakinoto, 2001).

4.2. Hodographs

A plot of composite hodographs seems to reveal distinct differences among the various supercell and derecho categories (Fig. 4). SF derecho events occur in stronger

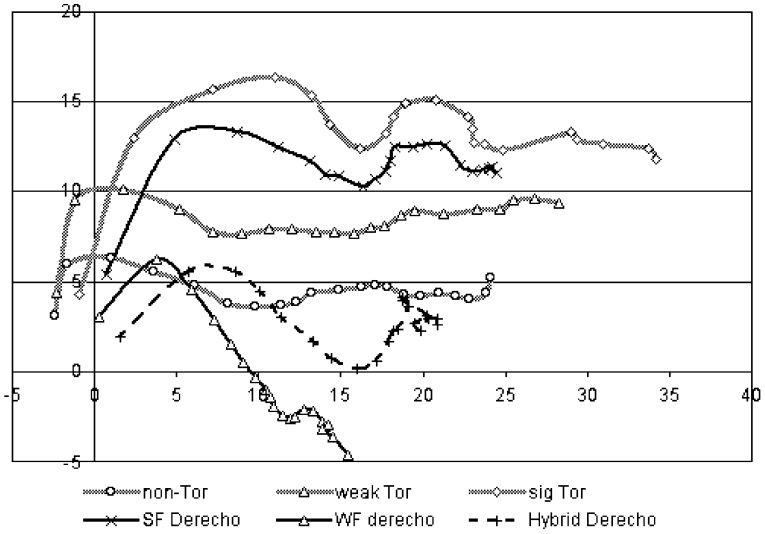

Fig. 4. Comparison of mean hodographs for the three supercell categories (non-tornadic, weak tornadic [< F2 rating], and significant [≥ F2 rating]), and the three derecho categories (SF, WF, and Hybrid) (see the key). Hodograph plot shows the *u*-component along the ordinate and the *v*-component along the abscissa (both m s^{-1}).

flow and shear than the hybrid and WF cases, and they have a much longer hodograph. This is also consistent with the findings about shear magnitude from ED01. The WF and hybrid hodograph plots are similar in structure below 4 km AGL; however, the hybrid cases are associated with stronger winds throughout the hodograph on average. In addition, the WF derechos indicate a pronounced northwest flow signal with near uniform, northwesterly flow in the midtroposphere (i.e., northwesterly 3–6 km AGL winds around 10 m s^{-1}), which is consistent with Johns and Hirt (1987).

Fig. 4 also indicates that significant tornadic supercell hodographs are much longer on average than hodographs for all other categories. The SF derechos and tornadic supercells occur in similar wind fields, with strong shear in the lowest 1 km AGL and pronounced clockwise turning in the lowest 3 km AGL, on average.

Just showing the mean hodographs is not sufficient, however. It is important to consider the *variability* of the hodographs when comparing the mean hodographs to one another. Although the mean hodographs suggest significant tornadic supercells occur in slightly stronger wind environments than SF derechos (Fig. 5), additional examination indicates that the mean SF derecho hodograph falls well within the middle 50% of all significant tornadic supercells in our dataset. This implies that hodographs of significant tornadic supercells and SF derechos can be very similar; distinguishing between the two events from hodograph structure alone could be quite problematic.

For the derechos, Fig. 6 reveals that the SF derecho mean hodograph is *outside* the 90th percentile for the WF derecho distribution, whereas the WF derecho mean is just *inside* of

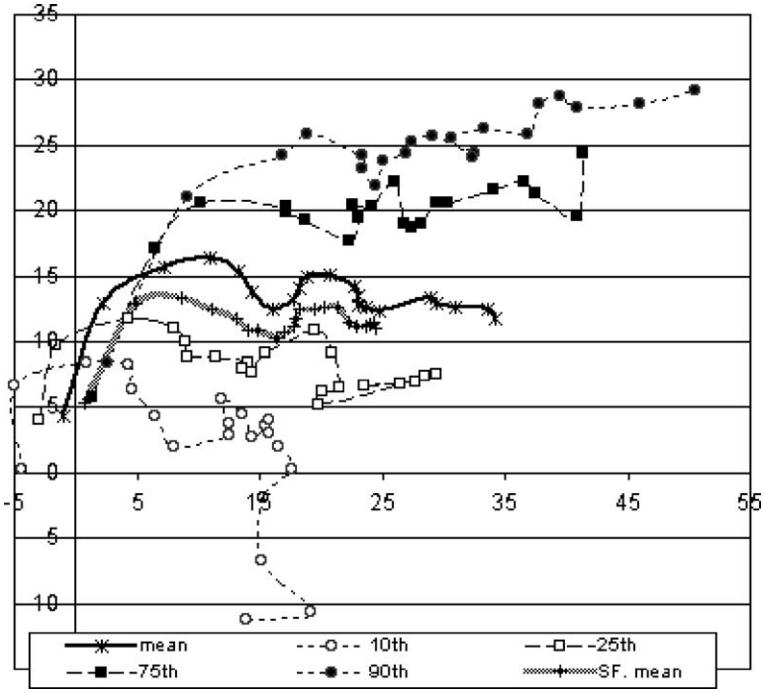

Fig. 5. Comparison plot of the 10th, 25th, mean, 75th, and 90th percentile hodoographs for supercells producing significant tornadoes (see the key), with the mean hodograph for SF derechos.

the 10th percentile of the SF derecho distribution (Fig. 7). This supports the suggestion that the hodographs for the SF and WF derechos are quite different at a high confidence level—these distributions do not overlap very much.

If we do a similar comparison of the supercell category hodographs, the mean hodograph for weak tornado-producing supercells is just inside of the 25th percentile of the distribution for the significant tornado-producing supercells (Fig. 8a).[4] Similarly, the mean hodograph for all tornadic supercells is just inside the 75th percentile for non-tornadic supercells (Fig. 8b). This suggests that the hodographs for tornadic supercells are distinguishable from non-tornadic supercells, although not with as high a confidence level as the distinction between SF and WF derecho hodographs. Also, the hodographs for significant tornado-producing supercells are comparably distinct from those for weak tornado-producing supercells. The overlap between the middle 50% of each distribution is not very great, and certainly the hodographs for significant tornado-producing supercells appear to be distinct from those for non-tornadic super-

[4] Comparing Fig. 8a to Fig. 5, it can be observed that the *mean* hodograph for significant tornadoes is quite similar to the *median*, indicating that the distributions are not strongly skewed. This result was found for virtually all the composite hodographs.

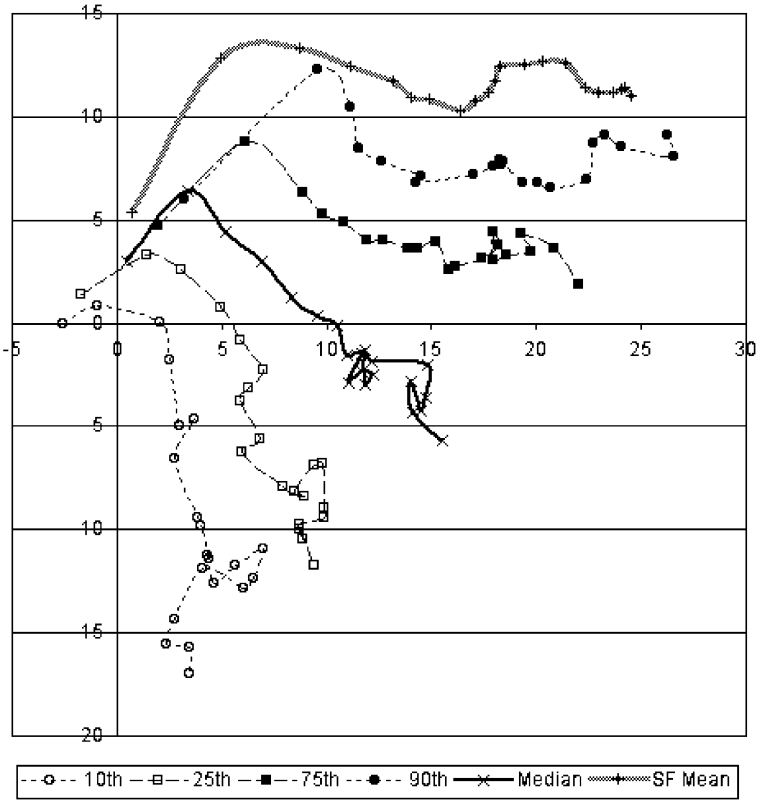

Fig. 6. Comparison plot of the 10th, 25th, 50th (median), 75th, and 90th percentile hodographs for WF derechos (see the key), with the mean hodograph for SF derechos.

cells. This result is consistent with the parameter comparisons to follow in Section 4.3.

When the hodographs are transformed to a storm-relative framework, using the observed storm motions (Fig. 9), it is apparent that derechos are associated with the strongest storm-relative inflow in the lowest 1 km AGL. Further, all derecho events (and, to the greatest extent, the WF cases) develop and persist in environments with *deep* system-relative inflow (front-to-rear flow) from the surface through 8–9 km AGL. This is likely to be related to the relatively fast movement of WF derechos, in comparison to their environmental wind fields (ED01). The tendency for *deep* front-to-rear flow in derechos may be related to the predominance of MCSs with trailing stratiform precipitation (Parker and Johnson, 2000) and the development of the so-called ''deep convergence zone'' noted by Lemon and Parker (1996).

In contrast, the supercell hodographs all show pronounced rear-to-front flow above 2–3 km AGL, especially for the significant tornado-producing supercells. This is markedly evident above 4 km AGL, where the supercell hodographs exhibit rear-to-front system-relative flow increasing through 10 km AGL.

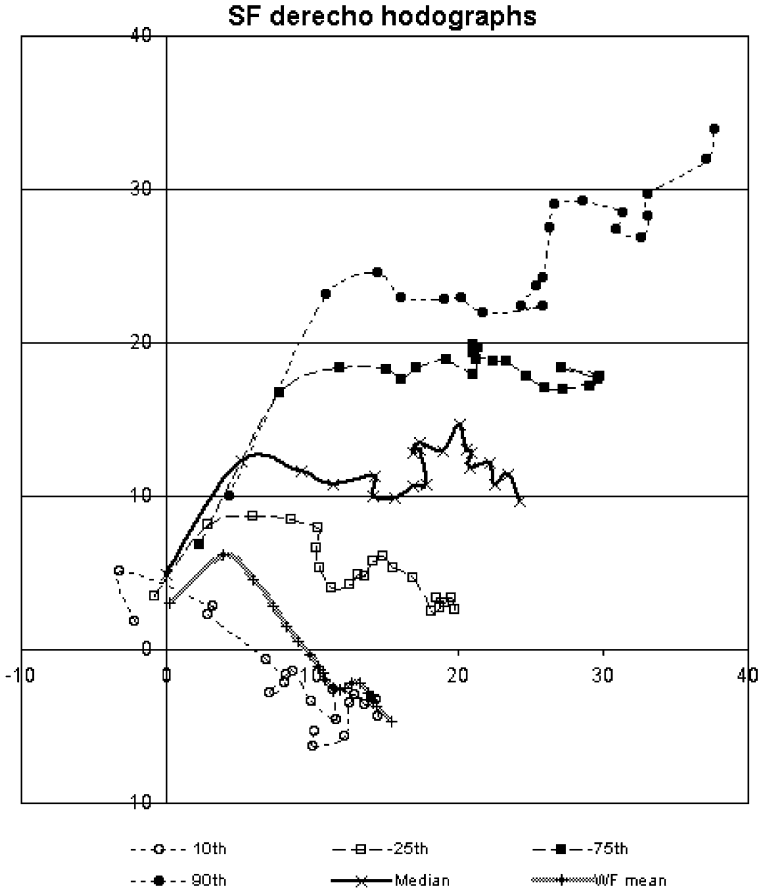

Fig. 7. Comparison plot of the 10th, 25th, 50th (median), 75th, and 90th percentile hodographs for SF derechos (see the key), with the mean hodograph for WF derechos.

4.3. Parameter comparisons

In this section, we extend some of the ED01 results to include some parameters not examined therein for the derecho proximity sounding data, as well as evaluating parameters for the supercell proximity soundings. This has been done to facilitate the comparison between the derechos and the supercells.

A plot of the 0–1 km shear (Fig. 10) comparing SF derechos with the supercells confirms the impressions gained from the hodograph comparisons. The SF derecho low-level shears are quite comparable with the shears associated with significant tornado-producing supercells. Furthermore, this parameter gives the impression that the three categories of supercells are associated with a progression of 0–1 km shear that increases monotonically from non-tornadic, through all tornadic, to significant tornado-producing

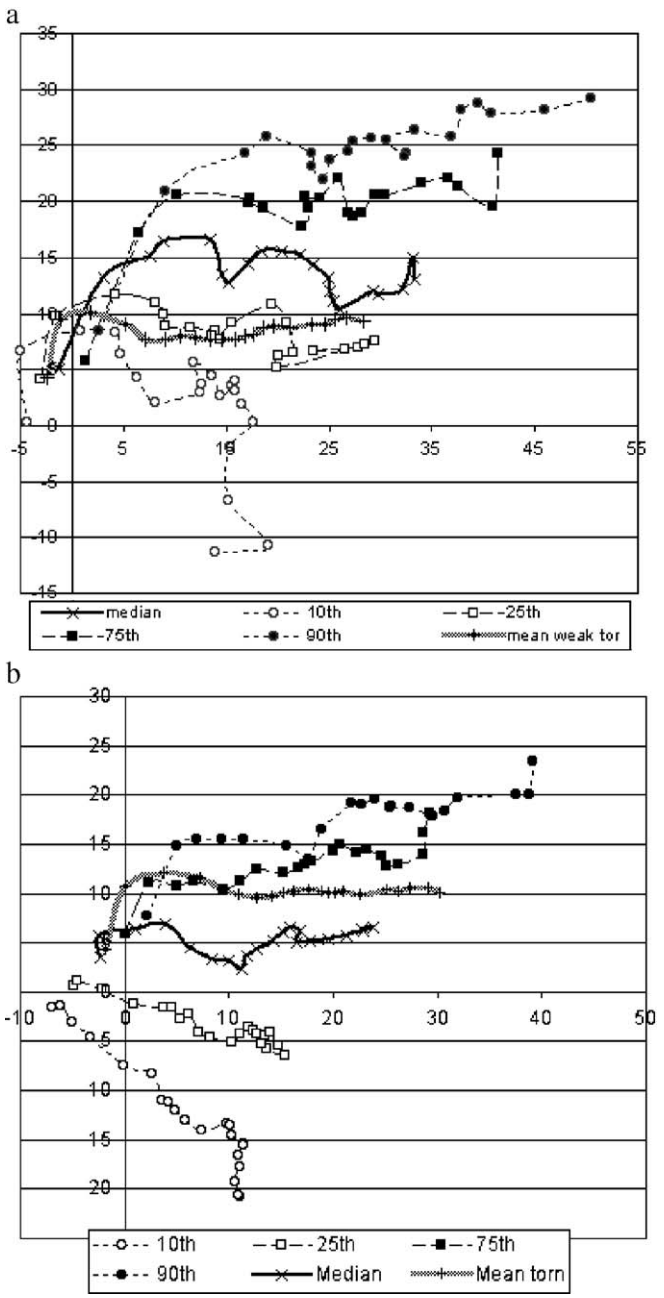

Fig. 8. (a) Comparison plot of the 10th, 25th, 50th (median), 75th, and 90th percentile hodographs for supercells producing significant tornadoes (see the key), and the mean hodograph for supercells producing weak tornadoes. (b) Comparison plot of the 10th, 25th, 50th (median), 75th, and 90th percentile hodographs for the non-tornadic supercells (see the key), and the mean hodograph for all tornadic supercells.

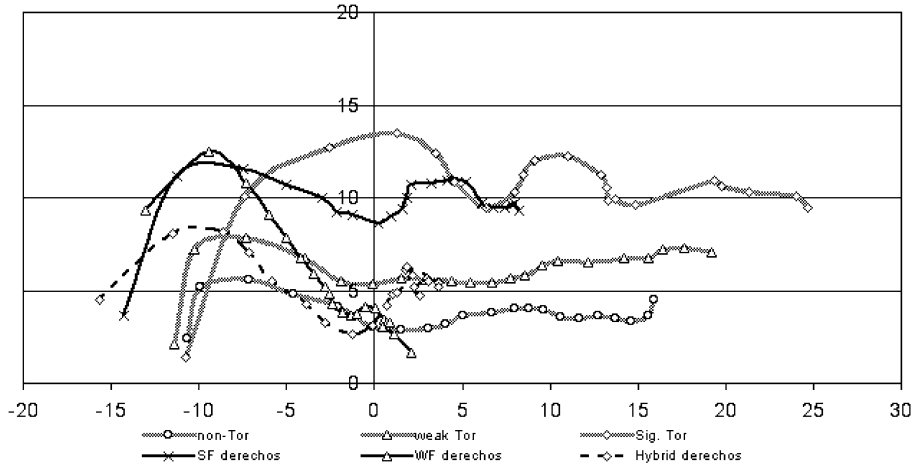

Fig. 9. As in Fig. 4, but using storm-relative winds, rather than ground-relative winds.

supercells, such that the overlap between the middle 50% of the distributions for non-tornadic versus significant tornado-producing supercells is negligible. Note that the mean 0–1 km shear for the significant tornado-producing supercells is somewhat larger than that for SF derechos, but this difference is not likely to be statistically significant, given the variability within the distributions.

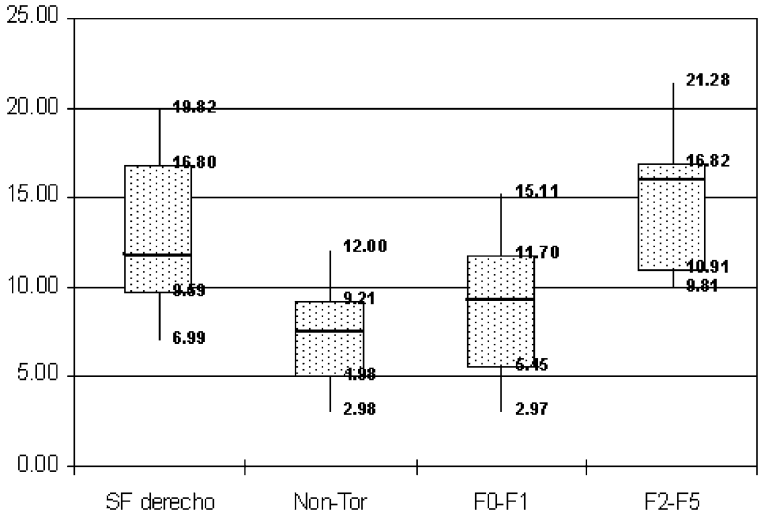

Fig. 10. 0–1 km (AGL) shear magnitude (m s^{-1}) box-and-whisker plots, showing the 10th, 25th, 75th, and 90th percentile values for the indicated categories, with the "box" containing the middle 50% of the distribution (between the 25th and 75th percentllles), while the "whiskers" denote the 10th and 90th percentiles. The median (50th percentile) is indicated by the heavy line within the box.

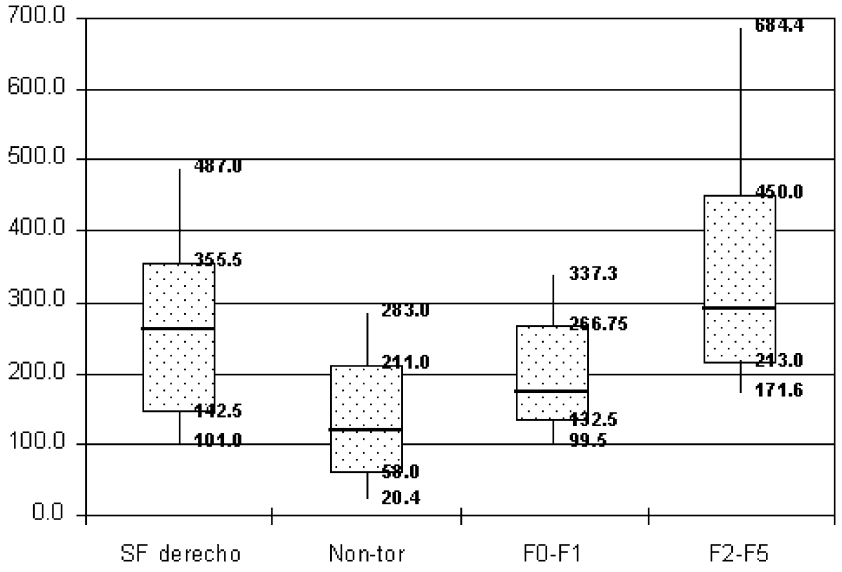

Fig. 11. As in Fig. 10, except for 0–3 km (AGL) storm relative helicity ($m^2\ s^{-2}$).

The 0–3 km storm-relative helicity (SRH; Fig. 11) also exhibits some apparent merit in distinguishing between the different supercell categories, especially between non-tornadic and significant tornadic events. However, the EHI (Fig. 12) appears to be best at distinguishing the tornadic versus non-tornadic supercell cases, with values in excess of

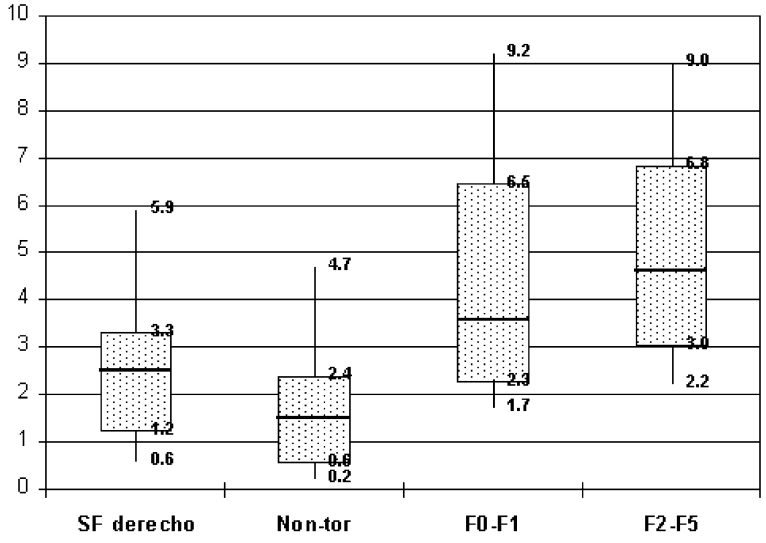

Fig. 12. As in Fig. 10, except for the dimensionless Energy–Helicity Index (EHI).

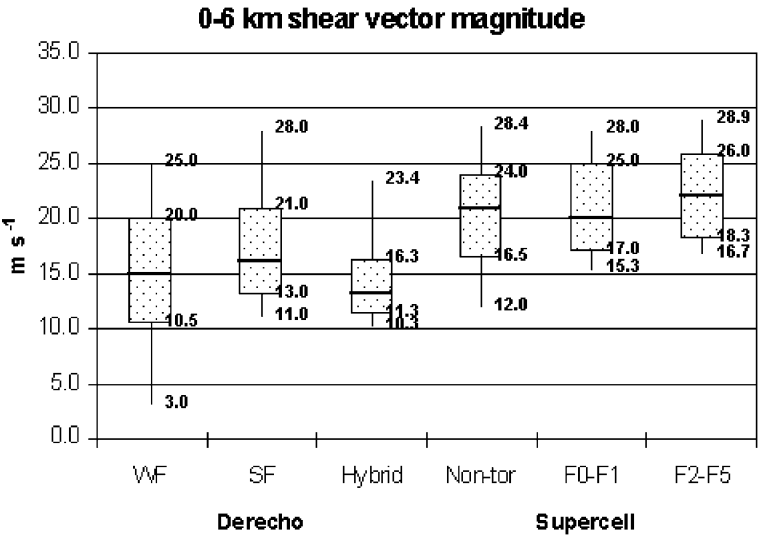

Fig. 13. As in Fig. 10, except for 0–6 km shear (m s^{-1}).

2.5 encompassing 75% of the tornado cases, but only 25% of the non-tornadic supercells. Observe also that the 0–3 km SRH distribution for SF derechos is within the supercell range for all supercell categories, whereas the EHI for SF derechos is similar only to the nontornadic supercells.

Neither 0–3 km AGL SRH or EHI show much promise for distinguishing between weak and significant tornado-producing supercells. The 0–1 km AGL shear (Fig. 10), however, clearly is the most useful in this regard; 10 m s^{-1} of 0–1 km shear separates the significant tornado-producing supercells from all but 25% of the other supercell categories.

The 0–6 km shear (Fig. 13) suggests that supercells occur in environments with slightly stronger deep layer shears than derechos, but the overlap among the distributions implies that this is probably not useful for forecasting purposes. Even this parameter suggests that derechos and supercells can occur within similar environments.

5. Discussion and conclusions

The result of this study seems to support the possibility of some capability for forecasting what *type* of supercell (non-tornadic, weak tornado-producing, or significant tornado-producing) or derecho (SF, WF, or hybrid) is likely. However, a broad similarity between derecho and supercell environments is also apparent. Parameters using some combination of CAPE and shear (such as the EHI) look promising to distinguish nontornadic and tornadic supercells. Low-level humidity and shear also appear to be able to discriminate between tornadic and significant tornado-producing supercells. SF and WF derecho environments are notably different, as was shown by ED01.

As indicated by the apparent difference in *storm-relative* flow between supercells and derechos, the large-scale organization of convection may be strongly associated with the distribution of hydrometeors *relative* to the persistent updrafts. Average storm-relative winds above 4 km AGL are noticeably different between derechos and discrete supercells. These results are consistent with studies that have found the distribution of hydrometers and precipitation is strongly influenced by the mid- and upper-level wind fields *relative* to the system's motion (Brooks et al., 1994, Thompson, 1998, Rasmussen and Straka, 1998, Parker and Johnson, 2000). This implies that the redistribution of precipitation to the rear of the leading line of convection is an important factor in derecho maintenance (especially in weakly forced cases). In contrast, rear-to-front (storm-relative) transport of hydrometeors at the middle and upper levels is characteristic of discrete supercells, at least within our relatively small sample. This is consistent with the classic studies of supercells. However, since forecasts are generally needed *before* the convection develops (and so the storm motion is not necessarily known in advance), these results still leave the forecaster with the challenge of predicting storm motion if the character of the convection is to be forecast. Reliable and highly accurate methods for forecasting storm motion remain to be developed.

Our results indicate that a number of additional factors, such as how the storms are initiated or how storms move relative to their point of initiation, may be needed to determine whether convection will develop and evolve as discrete or linear convection. If initiating mesoscale ascent is distributed more or less uniformly and strongly along a linear feature (such as a front, a dryline, or the outflow from earlier convection), and the convection stays tied to that linear initiating feature, this might favor derechos in preference to supercells. On the other hand, if existing linear features like fronts and drylines do not seem to have strong convergence and associated ascent, or the initial convection moves away from such a linear feature without producing a large cold pool, it might be that more subtle features leading to storm initiation (such as those discussed by Roebber et al., 2002) would result in discrete supercells instead of a derecho. It also seems likely that both types of events could occur in some situations and this is indeed consistent with the findings of ED01, wherein it was shown that many SF derechos also included reported tornadoes. Anecdotal forecaster experience suggests that both derechos and supercells can be present contemporaneously in what appear to be similar environments.

It is clear that important work remains to be done. For example, at this point, it is only speculation that the morphology of the initiating process is an important factor in the occurrence of derechos or discrete supercells in these similar environments. This hypothesis would need to be tested in future work. Further, it would be useful to continue to expand these proximity sounding datasets to improve the chances that the results are indeed representative. Increasing the number of cases would also permit the evaluation of any forecasting schemes on independent data—that is, forecasting schemes can be developed on some subset of the whole dataset and then tested on the remainder of the cases as an independent test. Further analysis of our results might include, for instance, a proper test of the statistical significance of the differences between the categories, as well as the determination of the best threshold values for our parameters to be using in developing forecasting techniques, including probabilistic forecasting schemes.

Perhaps the most optimistic interpretation of our results is that *probabilistic* forecasts of convective mode are possible. Using these composite sounding characteristics and parameters of the sort we have explored, in combination with some method for predicting storm motion, it might be possible to estimate the chances for the various convective modes, either probabilistically or using thresholds (e.g., similar to that done by Monteverdi et al., 2003). A quantitative evaluation of any such scheme would need to be done. The current study is simply one step toward developing forecast techniques to anticipate convective modes.

References

Brooks, H.E., Doswell III, C.A., Cooper, J., 1994. On the environments of tornadic and nontornadic mesocyclones. Weather Forecast. 9, 606–618.

Brown, R.A., 1993. A compositing approach for preserving significant features in atmospheric profiles. Mon. Weather Rev. 121, 874.

Corfidi, S.F., 1998. Forecasting MCS mode and motion. Preprints, 19th Conf. Severe Local Storms, Minneapolis, MN, Amer. Meteor., pp. 626–629.

Davies, J.M., 1993. Hourly helicity, instability, and EHI in forecasting supercell tornadoes. Preprints, 17th Conf. Severe Local Storms. St. Louis, MO. Amer. Meteor., pp. 107–111.

Evans, J.S., Doswell III, C.A., 2001. Examination of derecho environments using proximity soundings. Weather Forecast. 16, 329–342.

Evans, J.S., Doswell III, C.A., 2002. Investigating derecho and supercell proximity soundings. Preprints, 21st Conf. Severe Local Storms, San Antonio, TX. Amer. Meteor., pp. 635–638.

Gale, J.J., Gallus Jr., W.A., Jungbluth, K.A., 2002. Toward improved prediction of mesoscale convective system dissipation. Weather Forecast. 17, 856–872.

Johns, R.H., Hirt, W.D., 1987. Derechos: widespread convectively-induced windstorms. Weather Forecast. 2, 32–49.

Johns, R.H., Broyels, C., Eastlack, D., Guerrero, H., Harding, K., 2000. The role of synoptic patterns and temperature and moisture distribution in determining the locations of strong and violent tornado episodes in the north central united states: a preliminary examination. Preprints, 20th Conf. Severe Local Storms, Orlando, FL. Amer. Meteor. Soc., pp. 489–492.

Lemon, L.R., Parker, S., 1996. The Lahoma deep convergence zone: its characteristics and role in storm dynamics and severity. Preprints, 18th Conf. Severe Local Storms, San Francisco, CA. Amer. Meteor., pp. 70–75.

Markowski, P.M., Straka, J.M., Rasmussen, E.N., 2002. Direct surface thermodynamic observations within the rear-flank downdrafts of nontornadic and tornadic supercells. Mon. Weather Rev. 130, 1692–1721.

Monteverdi, J.P., Doswell III, C.A., Lipari, G.S., 2003. Shear parameter thresholds for forecasting California tornadic thunderstorms. Weather Forecast. 17, 357–370.

Parker, M.D., Johnson, R.H., 2000. Organizational modes of midlatitude mesoscale convective systems. Mon. Weather Rev. 128, 3413–3436.

Rasmussen, E.N., Blanchard, D.O., 1998. A baseline climatology of sounding-derived supercell and tornado forecast parameters. Weather Forecast. 13, 1148–1164.

Rasmussen, E.N., Straka, J.M., 1998. Variations in supercell morphology: Part I. Observations of the role of upper-level storm-relative flow. Mon. Weather Rev. 126, 2406–2421.

Roebber, P.J., Schultz, D.M., Romero, R., 2002. Synoptic regulation of the 3 May 1999 tornado outbreak. Weather Forecast. 17, 399–429.

Rotunno, R., Klemp, J.B., Weisman, M.L., 1988. A theory for strong, long-lived squall lines. J. Atmos. Sci. 45, 463–485.

Thompson, R.L., 1998. Eta model storm-relative winds associated with tornadic and nontornadic supercells. Weather Forecast. 13, 125–137.

Wakinoto, R.M., 2001. Convectively driven high wind events. Severe Convective Storms, Meteor. Monogr., 28, no. 50. Amer. Meteor. Soc., pp. 255–298.